

Rapid Report

Photolysis-induced suppression of inhibition in rat hippocampal CA1 pyramidal neurons

Jun Wang and Robert S. Zucker

Department of Molecular and Cell Biology, University of California, Berkeley, CA 94720, USA

(Received 20 March 2001; accepted after revision 3 May 2001)

1. Whole cell patch clamp recording, Ca^{2+} measurement with ratiometric fluorescent dyes and photolysis of caged Ca^{2+} were combined to investigate the depolarization- and photolysis-induced suppression of inhibition (DSI and PSI) in rat hippocampal CA1 pyramidal cells.
2. A 5-s depolarization from -70 mV to 0 mV or a 6-s photolysis of nitrophenyl-EGTA (NPE) in cell bodies could each depress the frequency of spontaneous inhibitory postsynaptic currents (IPSCs) and the amplitude of evoked IPSCs while elevating intracellular Ca^{2+} concentration ($[\text{Ca}^{2+}]_i$).
3. Within a cell the elevation of $[\text{Ca}^{2+}]_i$ induced by depolarization was inversely related to that induced by photolysis, suggesting that higher $[\text{NPE}]$ is more effective in releasing caged Ca^{2+} but also increases buffer capacity to reduce $[\text{Ca}^{2+}]_i$ rises caused by Ca^{2+} influx through voltage-dependent Ca^{2+} channels.
4. Both DSI and PSI were linearly related to $[\text{Ca}^{2+}]_i$, with a 50% reduction in transmission occurring at about 3.6–3.9 μM .
5. $[\text{Ca}^{2+}]_i$ recovered more quickly than DSI, indicating that the duration of DSI is not set simply by the duration of $[\text{Ca}^{2+}]_i$ elevation, but rather entails other rate-limiting processes.
6. We conclude that DSI is activated by micromolar $[\text{Ca}^{2+}]_i$ acting far from sites of Ca^{2+} entry through channels in the plasma membrane.

In hippocampal CA1 pyramidal cells and in cerebellar Purkinje cells, transient depolarization by brief trains of action potentials or voltage pulses suppresses inhibitory inputs to the depolarized cell. This phenomenon, known as depolarization-induced suppression of inhibition (DSI), depends upon Ca^{2+} influx through voltage-activated Ca^{2+} channels (Lenz *et al.* 1998) and appears to involve the production of a retrograde messenger in the postsynaptic neuron. The messenger, thought to be either glutamate (Glitsch *et al.* 1996; Morishita & Alger, 1999) or a cannabinoid (Wilson & Nicoll, 2001), then migrates to inhibitory presynaptic terminals to reduce both spontaneous and evoked GABA release to the depolarized cell (Pitler & Alger, 1992).

Ca^{2+} is necessary for the induction of DSI since DSI can be reduced or blocked by the introduction of EGTA or BAPTA into pyramidal cells (Lenz & Alger, 1999). It has not yet been shown, however, that a postsynaptic rise in $[\text{Ca}^{2+}]_i$ alone is sufficient to induce DSI. Nor has it been determined how high a $[\text{Ca}^{2+}]_i$ elevation is necessary to induce DSI. Recently, the $[\text{Ca}^{2+}]_i$ change accompanying

DSI in cerebellar Purkinje cells has been reported to be in the submicromolar range (Glitsch *et al.* 2000). However, the $[\text{Ca}^{2+}]_i$ increase induced by depolarization is not spatially homogeneous and the measurement reflects a volume-averaged Ca^{2+} elevation. It is not yet clear whether Ca^{2+} acts in a relatively local region of the postsynaptic cell at higher concentrations to activate DSI, or whether DSI is really sensitive to the more modest $[\text{Ca}^{2+}]_i$ changes measured globally.

We have used the ratiometric Ca^{2+} indicator BTC to measure volume-averaged $[\text{Ca}^{2+}]_i$ changes during depolarizations that induce DSI. We have also induced PSI directly by the spatially uniform photorelease of caged Ca^{2+} using the photosensitive Ca^{2+} chelator nitrophenyl-EGTA (NPE) (Ellis-Davies & Kaplan, 1994). Comparison of the Ca^{2+} dependence of suppression of inhibition induced by the two methods leads to the conclusion that DSI in CA1 pyramidal cells is activated by a postsynaptic rise in Ca^{2+} in the low micromolar range and that Ca^{2+} acts at a distance from sites of influx rather than in local microdomains of high $[\text{Ca}^{2+}]_i$.

METHODS

Slice preparation and electrophysiology

Transverse hippocampal slices, 300 μm thick, were cut with a Vibratome 1000 (TPI, St Louis, MO, USA) from brains of 11- to 22-day-old Sprague-Dawley rats after halothane anaesthesia and decapitation (Neveu & Zucker, 1996), using procedures approved by the institutional Animal Care and Use Committee. Before recording, slices were maintained for at least 1 h in recording medium containing (mM): 119 NaCl, 3 KCl, 2.5 CaCl₂, 2 MgSO₄, 1 NaH₂PO₄, 26 NaHCO₃, 10 D-glucose, saturated with 95% O₂-5% CO₂. They were then transferred to a recording chamber and perfused continuously at 2.5 ml min⁻¹ at 22°C. 2-Amino-5-phosphonovaleric acid (APV; 100 μM) and 6-cyano-7-nitroquinoxaline-2,3-dione (CNQX; 20 μM) were included in the recording solution.

A recording chamber was placed on a modified Nikon Optiphot microscope and cells were observed through a $\times 40$ water immersion objective lens (UV, NA 0.7, Olympus, Tokyo, Japan). Whole cell recording on CA1 pyramidal cells was performed with an SEC-05LX amplifier (npi electronic, Tamm, Germany). The recording pipettes had resistances of 2–4 M Ω when filled with (mM): 52 CsCH₃SO₃, 55 CsCl, 25 CsHepes, 3 MgCl₂, 5 QX-314Br, 5 K₄NPE, 2.5 CaCl₂, 0.3 BTC, 2 Na₂ATP, 0.3 NaGTP, pH 7.3 adjusted with HCl. All chemicals were obtained from Sigma (St Louis, MO, USA) except BTC and NPE (Molecular Probes, Eugene, OR, USA) and QX-314Br (Alomone Labs,

Jerusalem, Israel). IPSCs were recorded under voltage clamp, with cells held at -70 mV and corrected for a liquid junction potential measured at -5 mV. With our solutions, IPSCs have a reversal potential of -17 mV and so appear at -70 mV as an inward current. A bipolar stimulating electrode (glass pipette with tip diameter of ~ 4 μm , filled with recording medium, glued to a fine tungsten rod) was placed in or near CA1 stratum pyramidale. Test pulses were delivered every 5 s. IPSCs were digitized at 10 kHz and analysed with pCLAMP 8 (Axon Instruments, Union City, CA, USA). Recording was terminated whenever series resistance exceeded 40 M Ω or leakage current grew larger than 0.2 nA. DSI and PSI were calculated using the mean of the two IPSCs just before the depolarization or photolysis ($\text{amp}_{\text{baseline}}$) and the two IPSCs just after the depolarization or photolysis period (amp_{test}):

$$\text{DSI (or PSI) (\%)} = 100(1 - (\text{amp}_{\text{test}}/\text{amp}_{\text{baseline}})).$$

Data are expressed as means \pm S.E.M.

Photolysis of caged Ca²⁺ and [Ca²⁺]_i measurement

A Polychrome IV multi-wavelength monochromator (T.I.L.L. Photonics, Munich, Germany) was used for both the UV light source for photolysis and the excitation light source for Ca²⁺ imaging. Monochromatic light beams were coupled to the microscope via a light guide using a T.I.L.L. epifluorescence condenser. Fluorescent light emitted from the cell was captured using a cooled-CCD camera

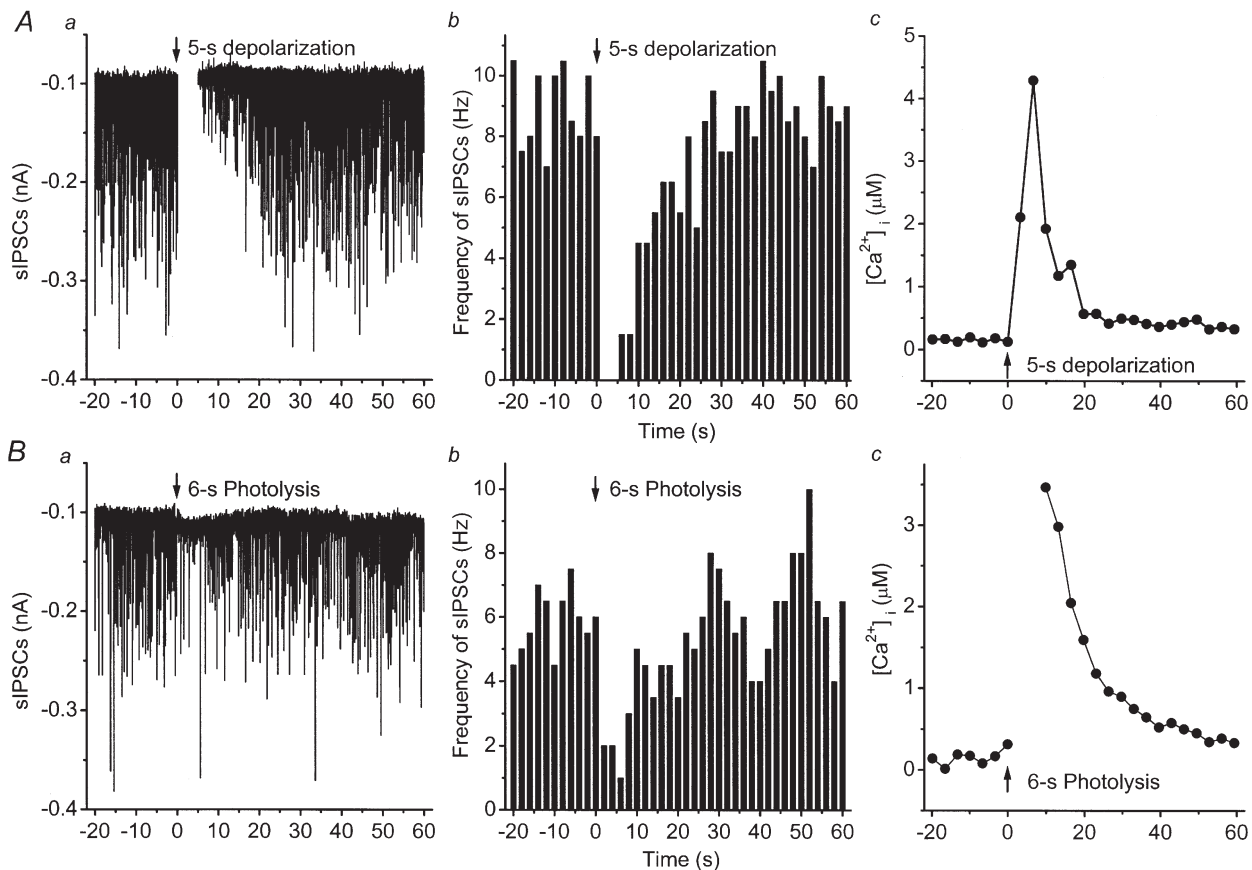


Figure 1. Depolarization- and photolysis-induced [Ca²⁺]_i increase and suppression of spontaneous IPSCs (sIPSCs)

A, DSI and [Ca²⁺]_i increase; *B*, PSI and [Ca²⁺]_i increase. Left panels show effects of a 5-s depolarization to 0 mV (top row), or a 6-s photolysis (bottom row) on spontaneous IPSCs; centre panels show time courses of changes in frequencies of spontaneous IPSCs in 2-s bins. Right panels shows the [Ca²⁺]_i increase. Arrows mark the beginning of the depolarization or photolysis (at time 0).

(Sensicam, PCO Computer Optics, Kelheim, Germany). Axon Imaging Workbench 4 (Axon Instruments) controlled the camera and monochromator for Ca^{2+} imaging, while TILLADCC software (T.I.L.L. Photonics) controlled the Polychrome monochromator for photolysis at 360 nm. Exposures lasting 6 s were used, which we calculate should have photolysed 75% of the NPE in cells located 100 μm below the surface of the slice. This estimate took account of our measurement of hippocampal slice absorbance at 360 nm (decadic absorbance coefficient of 3 mm^{-1} , i.e. transmission drops 3 \log_{10} units or 1000-fold in 1 mm), and calibrations of the photolysis efficiency of the illumination through the microscope (Zucker, 1994).

For ratiometric imaging, two images were captured successively at excitation wavelengths of 400 and 480 nm, using a 505 nm dichroic mirror with extended UV reflectance and a $535 \pm 20 \text{ nm}$ emission filter (Chroma Technology, Brattleboro, VT, USA). Sample intervals ranged from 1.5 to 3.3 s. Ratios of fluorescence intensities were calculated after subtracting background fluorescence from neighbouring unstained portions of the slice. $[\text{Ca}^{2+}]_i$ was estimated on-line according to eqn (5) of Grynkiewicz *et al.* (1985). The soma region was chosen for analysis.

Calibration of BTC was performed according to procedures described previously (Ohnuma *et al.* 2001). Briefly, solutions resembling cytoplasm were prepared containing 15 mM DPTA (1,3-diaminopropan-2-ol-tetraacetic acid) to regulate $[\text{Ca}^{2+}]_i$, 50 mM CsHepes to regulate pH at pH 7.3, 5 mM fully Ca^{2+} -loaded NPE, 10 mM KCl (produced on neutralizing NPE), 0.3 mM BTC, 5 mM QX-314Br, and sufficient CsCl (24–75 mM) to keep the ionic strength constant at 158 mM. Ca^{2+} -free solution contained Ca^{2+} -free NPE and 10 mM EGTA instead of DPTA, while high- Ca^{2+} solution contained an excess of 10 mM CaCl_2 . In solutions of intermediate $[\text{Ca}^{2+}]_i$ (10, 25, 55 and 135 μM), DPTA was loaded with 20, 40, 60 and 80% Ca^{2+} , respectively. Free $[\text{Ca}^{2+}]_i$ was calculated by solving buffer equations for total amounts of DPTA, NPE, BTC and Ca^{2+} , assuming K_D values for NPE and BTC of 50 nM (Ellis-Davies & Kaplan, 1994) and 10 μM (Iatridou *et al.* 1994), respectively. The K_D of our sample of DPTA was measured as 40 μM at pH 7.3 from a plot of $[\text{Ca}^{2+}]_i$ vs. $[\text{Cs}_2\text{CaDPTA}]/[\text{Cs}_3\text{HDPTA}]$, using Ca^{2+} -selective electrodes in solutions identical to the calibration solutions without NPE and BTC and adjusted to 158 mM ionic strength.

The fluorescence ratio (F_{400}/F_{480}) for excitation wavelengths of 400 and 480 nm of each of the calibration solutions was measured in microcuvettes with 20 μm pathlength (VitroCom, Mountain Lakes, NJ, USA). A plot of $\log([\text{Ca-BTC}]/[\text{BTC}])$, calculated from the fluorescence ratio according to Grynkiewicz *et al.* (1985), vs. $\log([\text{Ca}^{2+}]_i)$ generates a linear curve which was used to calculate the K_D of Ca^{2+} binding to BTC as 7.4 μM in our ionic conditions and pH. This is very close to values reported previously (Iatridou *et al.* 1994) and is the value used in converting our ratiometric fluorescence measurements to calculate $[\text{Ca}^{2+}]_i$. Plotting fluorescence ratio vs. $\log([\text{Ca}^{2+}]_i)$ and using non-linear least squares fitting to the binding equation yielded an estimated K_D of 11 μM , consistent with earlier reports that this method of curve fitting generates higher estimates of K_D (Zhao *et al.* 1996). This range of K_D values gives some indication of the uncertainty in our estimates of the absolute magnitudes of $[\text{Ca}^{2+}]_i$.

RESULTS

Suppression of spontaneous IPSCs to $[\text{Ca}^{2+}]_i$ elevations evoked by depolarization or caged Ca^{2+} photolysis

Initially we determined that we are able to suppress inhibition by both photolysis of NPE and depolarization. Figure 1 illustrates examples of DSI and PSI measured as

a reduction in the frequency of spontaneously occurring IPSCs. It has been shown previously (Pitler & Alger, 1992; Alger *et al.* 1996) that these IPSCs are blocked by tetrodotoxin and therefore are due to IPSCs evoked by spontaneously occurring action potentials in presynaptic inhibitory interneurons. The left-hand panels show continuous current recordings from two different cells; the cell in the top row was depolarized to 0 mV for 5 s while the cell in the bottom row was photolysed at 360 nm for 6 s. Both procedures suppressed the spontaneously occurring IPSCs for about 20 s. The centre panels plot the frequencies of spontaneous IPSCs, while the right-hand panels display the concomitant $[\text{Ca}^{2+}]_i$ elevations in the cell bodies.

Caged Ca^{2+} acts as a Ca^{2+} buffer

Our success at suppressing inhibition by depolarization might seem surprising because NPE is a Ca^{2+} buffer similar to EGTA and it has been shown that EGTA perfused into CA1 pyramidal cells can block the induction of DSI (Lenz & Alger, 1999). However, complete block of DSI only occurred at an $[\text{EGTA}]$ of 10 mM, while our pipette solution contained only 2.5 mM of uncomplexed NPE. When 2 mM EGTA or BAPTA was perfused into cells, DSI could still be induced, albeit with somewhat longer depolarizations. Thus we would expect NPE to reduce, but not completely block, DSI.

An additional complication is that the ability to fill cells by perfusion from a patch pipette is variable, and we

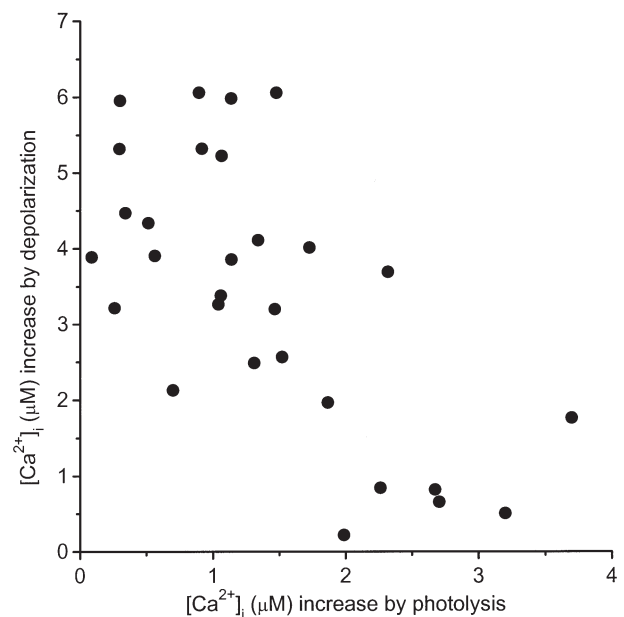


Figure 2. Inverse relationship between $[\text{Ca}^{2+}]_i$ elevated by depolarization and by photolysis

Each point represents the peak $[\text{Ca}^{2+}]_i$ level reached in a cell depolarized to 0 mV for 5 s (ordinate) vs. the peak $[\text{Ca}^{2+}]_i$ level caused by 6 s of photolysis (abscissa) in the same cell. The data were negatively correlated ($r = 0.66$) with slope -1.29 ± 0.28 .

suspected that the actual concentration of NPE achieved was not the same in all experiments. In that case, in some cells filled with higher intracellular concentrations of NPE, photolysis would be more effective in elevating $[Ca^{2+}]_i$, while in those same cells depolarization would be less effective because of the increased Ca^{2+} buffering. In other cells less effectively filled with NPE, we would expect less of an effect of photolysis on $[Ca^{2+}]_i$, while depolarization would more readily elevate $[Ca^{2+}]_i$. This led us to predict an inverse relationship between $[Ca^{2+}]_i$ elevation in response to depolarization and that in response to photolysis. Figure 2 confirms this prediction.

Suppression of evoked IPSCs

DSI may also be measured as a reduction in monosynaptic IPSCs evoked by stimulation of inhibitory interneurons in nearby stratum pyramidale. Figure 3 illustrates the effects in two different cells of depolarization (top row) or

photolysis (bottom row) on IPSC amplitudes evoked every 5 s, overlaid on the time course of changes in $[Ca^{2+}]_i$. Sample IPSCs are also shown. We found this method of measuring DSI to be more precise, in that IPSC amplitudes were inherently less variable than estimates of spontaneous IPSC frequency; thus estimates of both the magnitude and time course of DSI were more accurate. We restricted our analysis to this form of DSI.

Ca^{2+} dependence of suppression of inhibition evoked by depolarization and photolysis

Our main goal was to compare the Ca^{2+} sensitivities of depolarization- and photolysis-induced suppression of inhibition. The collected results of all experiments in which a clearly measurable DSI or PSI was observed appear in Fig. 4A and B. In order to obtain an extended range of $[Ca^{2+}]_i$ changes, we varied the duration of photolysis between 2 and 6 s or the depolarization

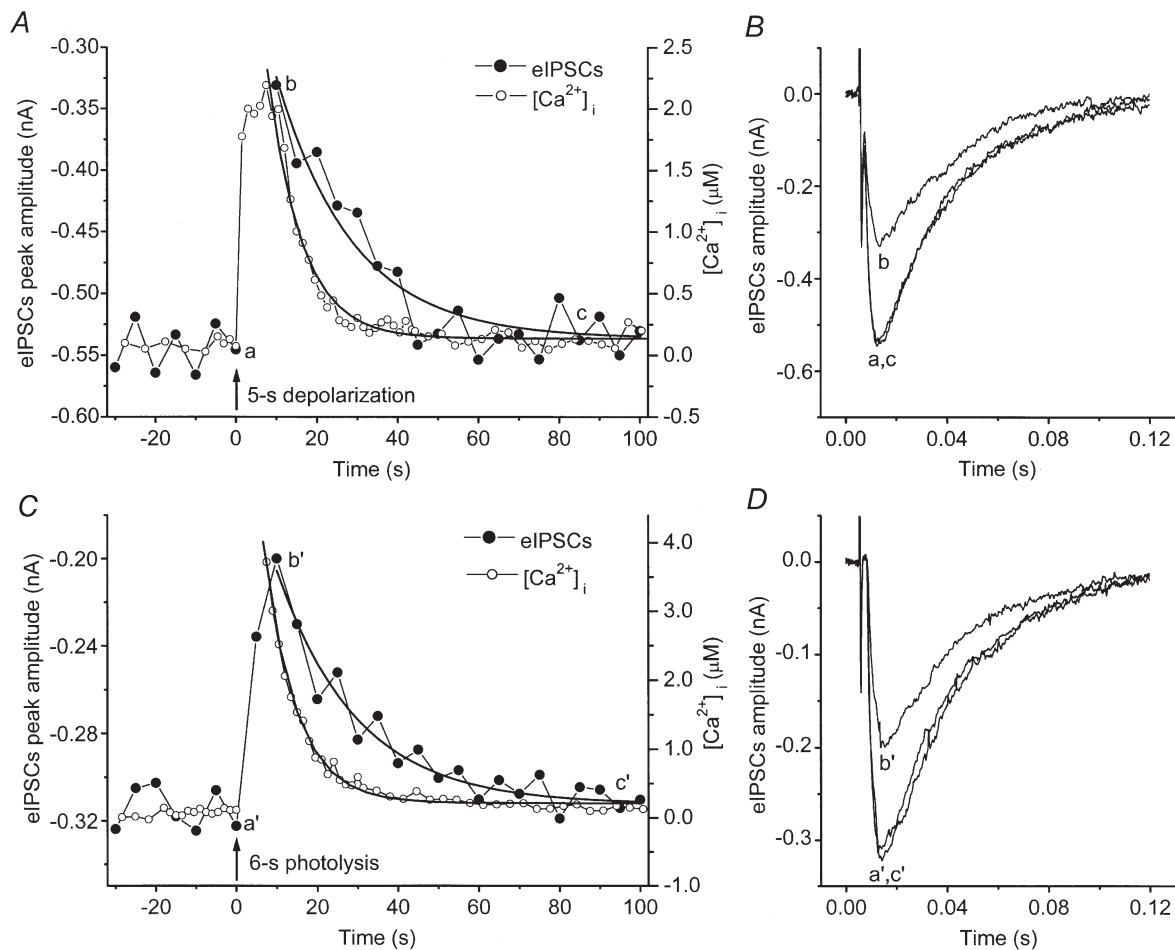


Figure 3. Depolarization- and photolysis-induced $[Ca^{2+}]_i$ increase and suppression of evoked IPSCs (eIPSCs)

A, depolarization-induced $[Ca^{2+}]_i$ (O) and DSI (●); lines drawn through data points are generated by single exponential fits. The recovery from DSI occurs more slowly ($\tau = 18.7 \pm 2.6$ s) than the recovery of $[Ca^{2+}]_i$ ($\tau = 8.3 \pm 0.4$ s). B, IPSCs before (a in A), during (b in A) and after (c in A) a 5-s depolarization. C, photolysis-induced $[Ca^{2+}]_i$ (O) and PSI (●). D, IPSCs before (a' in C), during (b' in C) and after (c' in C) a 6-s photolysis. Recovery from PSI takes longer ($\tau = 19.6 \pm 2.7$ s) than that of $[Ca^{2+}]_i$ ($\tau = 8.0 \pm 0.2$ s). Arrows mark the beginning of 5-s depolarization or 6-s photolysis (at time 0).

between 1 and 5 s in different experiments. In both types of experiment, increased elevation of $[Ca^{2+}]_i$ induced stronger DSI or PSI. Fitting the percentage of suppression *vs.* $[Ca^{2+}]_i$ to the Hill equation showed the Ca^{2+} dependence of suppression to be similar for both methods of $[Ca^{2+}]_i$ elevation.

Estimates of the Hill coefficient are made more accurately from a transformation of the data which plots the logarithm of $DSI/(DSI_{max} - DSI)$ *vs.* the logarithm of $[Ca^{2+}]_i$, where DSI_{max} is the maximum level of DSI. PSI data were transformed using a similar formula, replacing DSI with PSI. DSI_{max} was estimated by least squares fitting to the Hill equation to be $73 \pm 59\%$ for depolarization, while PSI_{max} was $63 \pm 27\%$ for photolysis. These estimates for the maximum levels of DSI and PSI are similar to those obtained previously for depolarization (Lenz & Alger, 1999). After transforming the data, the

Hill coefficients were 1.36 ± 0.25 for depolarization and 1.45 ± 0.27 for photolysis. IPSPs were reduced by half at $[Ca^{2+}]_i$ values of $3.9 \pm 0.5 \mu M$ for depolarization and $3.6 \pm 0.7 \mu M$ for photolysis. Covariance analysis demonstrated no significant difference between the two data sets ($P > 0.5$), indicating that DSI and PSI are identically affected by elevating $[Ca^{2+}]_i$ as a result of localized influx through voltage-gated Ca^{2+} channels and by the globally uniform elevation caused by caged Ca^{2+} photolysis.

DSI and PSI decay more slowly than $[Ca^{2+}]_i$

In the experiments illustrated in Fig. 3, recovery from DSI and PSI lasted longer (19 s) than the recovery of $[Ca^{2+}]_i$ from its peak value (8 s). To determine whether this was a consistent property of DSI and PSI, we plotted time constants of recovery from DSI or PSI and of $[Ca^{2+}]_i$

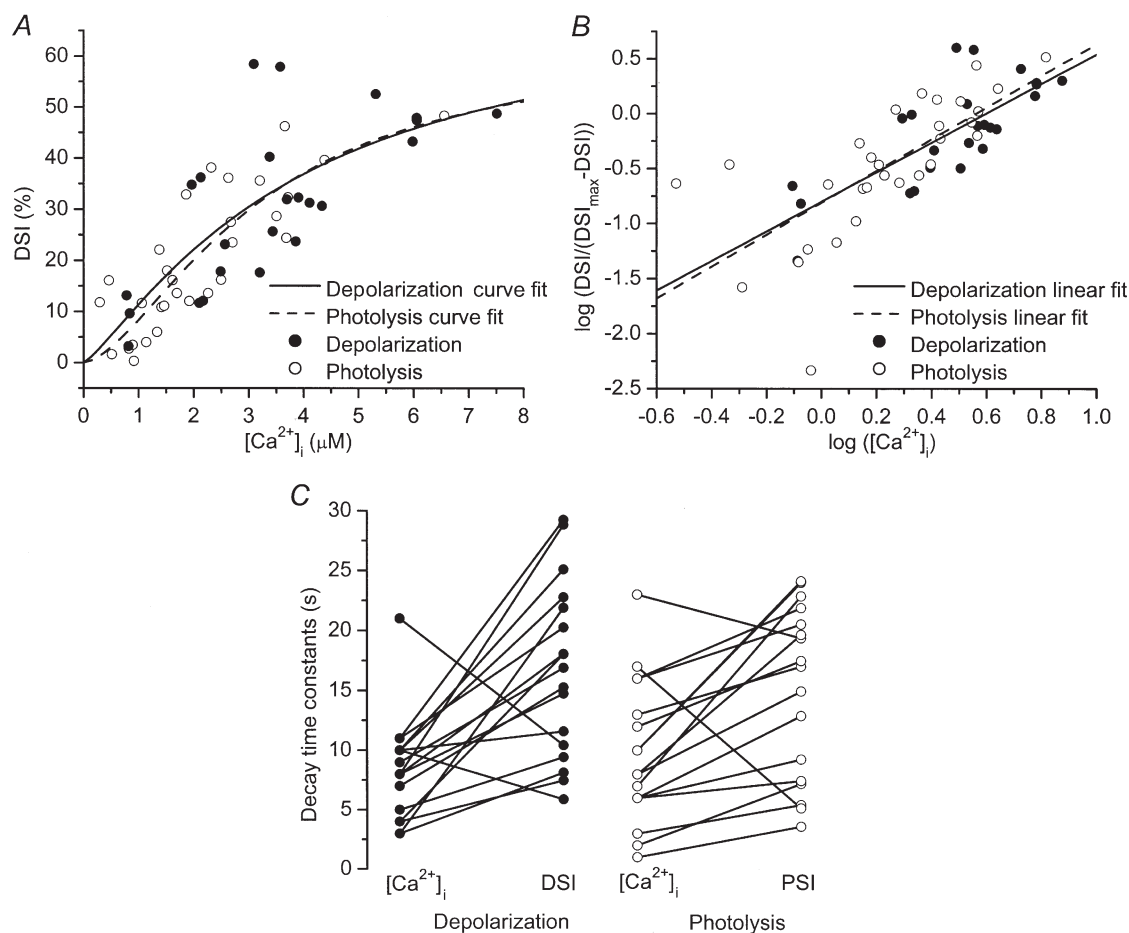


Figure 4. $[Ca^{2+}]_i$ dependence and decay rates of DSI and PSI

A and B show peak DSI (or PSI) of evoked IPSCs plotted *vs.* peak $[Ca^{2+}]_i$. $[Ca^{2+}]_i$ rises were obtained by varying the duration of depolarization or photolysis. A, continuous and dashed lines correspond to the fits of the data points to the Hill equation: $DSI = DSI_{max}([Ca^{2+}]_i)^n / (K_{50}^n + ([Ca^{2+}]_i)^n)$. For photolysis experiments, an identical equation was used with PSI replacing DSI. B, linear fit of the data points after logarithmic transformation. These two lines are not statistically different ($P > 0.5$, covariance analysis). Numbers of measurements: 24 for depolarization and 30 for photolysis. C, the left panel shows decay time constants (τ_{decay}) for DSI and $[Ca^{2+}]_i$ (16.7 ± 1.8 and 8.4 ± 1.0 s, respectively, $n = 17$). The right panel shows τ_{decay} for PSI and $[Ca^{2+}]_i$ (14.9 ± 1.8 and 9.7 ± 1.4 s, respectively, $n = 17$).

for each experiment in which suppression of inhibition was large enough ($\geq 15\%$) to give an exponential fit to its decay (Fig. 4C). In both types of experiment, suppression of inhibition lasted significantly longer than the $[Ca^{2+}]_i$ elevation ($P < 0.05$, sign test).

DISCUSSION

DSI is a form of communication between neurons that involves some sort of retrograde messenger released or expressed by the postsynaptic cell (Vincent & Marty, 1993; Alger *et al.* 1996). In both pyramidal and Purkinje neurons, DSI is mediated by Ca^{2+} influx through postsynaptic voltage-dependent Ca^{2+} channels and depends on an elevation in postsynaptic $[Ca^{2+}]_i$ (Pitler & Alger, 1992; Lenz & Alger, 1999; Glitsch *et al.* 2000). An obvious possibility is that the retrograde messenger in DSI is secreted in a Ca^{2+} -dependent fashion in a manner similar to neurotransmitter release or hormonal secretion. These forms of secretion involve a cooperative action of Ca^{2+} ions acting locally in microdomains near their points of entry through voltage-sensitive Ca^{2+} channels (Zucker, 1996). The cooperativity is reflected in a highly non-linear relationship between transmission and $[Ca^{2+}]_i$ (Dodge & Rahamimoff, 1967). The local action of Ca^{2+} is inferred from the fact that action potentials trigger secretion accompanied by a very small rise in global or volume-averaged presynaptic $[Ca^{2+}]_i$ (Charlton *et al.* 1982; von Gersdorff & Matthews, 1994; Tang *et al.* 2000), while $[Ca^{2+}]_i$ must be raised to between 1000 and 10 000 times higher levels by photolysis of photosensitive chelators to trigger rates of secretion similar to those occurring in an action potential (Delaney & Zucker, 1990; Zucker, 1993; Heidelberger *et al.* 1994; Heinemann *et al.* 1994; Landò & Zucker, 1994).

This situation contrasts dramatically with what we observe for DSI and PSI. The magnitude of suppression depends linearly on the magnitude of $[Ca^{2+}]_i$, whether elevated by caged Ca^{2+} photolysis or by depolarization. This is consistent with the finding that the magnitude of DSI is linearly related to the amount of Ca^{2+} influx (Lenz & Alger, 1999). We see no sign of a highly cooperative step between Ca^{2+} influx and suppression of inhibition. In our experiments, the $[Ca^{2+}]_i$ released by photolysis and needed to achieve a given magnitude of PSI is just the same as the volume-averaged $[Ca^{2+}]_i$ recorded when depolarization and Ca^{2+} entry through Ca^{2+} channels activates DSI. Thus there is no sign of Ca^{2+} acting locally in highly concentrated microdomains to elicit DSI. One indication of some degree of regional specialization in the activation of DSI by Ca^{2+} is that DSI is more sensitive to Ca^{2+} entry through N- and L-type channels than P- or Q-type channels (Lenz *et al.* 1998). This may reflect the relative prevalence of different channel types in somatic *vs.* dendritic membrane.

These results are consistent with other reports indicating that Ca^{2+} does not act locally in activating DSI – the slow-acting buffer EGTA and the much faster-acting buffer BAPTA are similar in their effectiveness in blocking DSI (Lenz & Alger, 1999; Glitsch *et al.* 2000). Another important difference between DSI and transmitter secretion is that DSI is not sensitive to specific toxin inhibitors of the SNARE complex involved in vesicle fusion (Wilson & Nicoll, 2001). One possibility is that $[Ca^{2+}]_i$ activates synthesis of a cannabinoid retrograde messenger, since it has been shown that cannabinoid synthetic enzymes are activated by $[Ca^{2+}]_i$ in the micromolar or even submicromolar range (Cadas *et al.* 1996).

We found that DSI and PSI last longer (time constant ~ 15 s, similar to that reported by Lenz & Alger, 1999) than the $[Ca^{2+}]_i$ rise that elicits it (time constant ~ 9 s). Our somatic $[Ca^{2+}]_i$ transients decay slightly more slowly than those reported previously (Regehr & Tank, 1992; Jaffe *et al.* 1994), probably because of the additional Ca^{2+} buffering provided by NPE. Our results indicate that slower processes downstream of Ca^{2+} influx determine the duration of DSI and PSI. Possibilities include retrograde messenger synthetic processes in the pyramidal cells (Cadas *et al.* 1996) and G-protein-activated enzymatic pathways in the presynaptic neurons (Pitler & Alger, 1994).

Our results in CA1 pyramidal cells may be compared with what is known about DSI in cerebellar Purkinje neurons (Glitsch *et al.* 2000). In Purkinje cells, a DSI of 50% was achieved with depolarizations leading to a volume-averaged $[Ca^{2+}]_i$ of only about 40 nM, compared to our value of almost 4 μ M. Thus cerebellar DSI appears to be more than one hundred times more sensitive to $[Ca^{2+}]_i$ than cortical DSI. In Purkinje cells, the relation between $[Ca^{2+}]_i$ and DSI was linear, as in cortex. However, in Purkinje cells a larger $[Ca^{2+}]_i$ rise could reflect the recruitment of additional Ca^{2+} channels in response to longer or larger numbers of pulses, rather than a change in local $[Ca^{2+}]_i$ in microdomains. In such microdomains DSI could be activated at higher concentrations than are indicated by volume-averaged $[Ca^{2+}]_i$ measurements. Additional experiments are needed to determine whether Ca^{2+} acts locally or globally to cause DSI in Purkinje cells.

ALGER, B. E., PITLER, T. A., WAGNER, J. J., MARTIN, L. A., MORISHITA, W., KIROV, S. A. & LENZ, R. A. (1996). Retrograde signalling in depolarization-induced suppression of inhibition in rat hippocampal CA1 cells. *Journal of Physiology* **496**, 197–209.

CADAS, H., GAILLET, S., BELTRAMO, M., VENANCE, L. & PIOMELLI, D. (1996). Biosynthesis of an endogenous cannabinoid precursor in neurons and its control by calcium and cAMP. *Journal of Neuroscience* **16**, 3934–3942.

- CHARLTON, M. P., SMITH, S. J. & ZUCKER, R. S. (1982). Role of presynaptic calcium ions and channels in synaptic facilitation and depression at the squid giant synapse. *Journal of Physiology* **323**, 173–193.
- DELANEY, K. R. & ZUCKER, R. S. (1990). Calcium released by photolysis of DM-nitrophen stimulates transmitter release at squid giant synapse. *Journal of Physiology* **426**, 473–498.
- DODGE, F. A. JR & RAHAMIMOFF, R. (1967). Co-operative action a calcium ions in transmitter release at the neuromuscular junction. *Journal of Physiology* **193**, 419–432.
- ELLIS-DAVIES, G. C. & KAPLAN, J. H. (1994). Nitrophenyl-EGTA, a photolabile chelator that selectively binds Ca^{2+} with high affinity and releases it rapidly upon photolysis. *Proceedings of the National Academy of Sciences of the USA* **91**, 187–191.
- GLITSCH, M., LLANO, I. & MARTY, A. (1996). Glutamate as a candidate retrograde messenger at interneurone-Purkinje cell synapses of rat cerebellum. *Journal of Physiology* **497**, 531–537.
- GLITSCH, M., PARRA, P. & LLANO, I. (2000). The retrograde inhibition of IPSCs in rat cerebellar Purkinje cells is highly sensitive to intracellular Ca^{2+} . *European Journal of Neuroscience* **12**, 987–993.
- GRYNKIEWICZ, G., POENIE, M. & TSIEN, R. Y. (1985). A new generation of Ca^{2+} indicators with greatly improved fluorescence properties. *Journal of Biological Chemistry* **260**, 3440–3450.
- HEIDELBERGER, R., HEINEMANN, C., NEHER, E. & MATTHEWS, G. (1994). Calcium dependence of the rate of exocytosis in a synaptic terminal. *Nature* **371**, 513–515.
- HEINEMANN, C., CHOW, R. H., NEHER, E. & ZUCKER, R. S. (1994). Kinetics of the secretory response in bovine chromaffin cells following flash photolysis of caged Ca^{2+} . *Biophysical Journal* **67**, 2546–2557.
- IATRIDOU, H., FOUKARAKI, E., KUHN, M. A., MARCUS, E. M., HAUGLAND, R. P. & KATERINPOULOS, H. E. (1994). The development of a new family of intracellular calcium probes. *Cell Calcium* **15**, 190–198.
- JAFFE, D. B., ROSS, W. N., LISMAN, J. E., LASSER-ROSS, N., MIYAKAWA, H. & JOHNSTON, D. (1994). A model for dendritic Ca^{2+} accumulation in hippocampal pyramidal neurons based on fluorescence imaging measurements. *Journal of Neurophysiology* **71**, 1065–1077.
- LANDÒ, L. & ZUCKER, R. S. (1994). Ca^{2+} cooperativity in neurosecretion measured using photolabile Ca^{2+} chelators. *Journal of Neurophysiology* **72**, 825–830.
- LENZ, R. A. & ALGER, B. E. (1999). Calcium dependence of depolarization-induced suppression of inhibition in rat hippocampal CA1 pyramidal neurons. *Journal of Physiology* **521**, 147–157.
- LENZ, R. A., WAGNER, J. J. & ALGER, B. E. (1998). N- and L-type calcium channel involvement in depolarization-induced suppression of inhibition in rat hippocampal CA1 cells. *Journal of Physiology* **512**, 61–73.
- MORISHITA, W. & ALGER, B. E. (1999). Evidence for endogenous excitatory amino acids as mediators in DSI of GABA_Aergic transmission in hippocampal CA1. *Journal of Neurophysiology* **82**, 2556–2564.
- NEVEU, D. & ZUCKER, R. S. (1996). Postsynaptic levels of $[\text{Ca}^{2+}]_i$ needed to trigger LTD and LTP. *Nature* **16**, 619–629.
- OHNUMA, K., WHIM, M. D., FETTER, R. D., KACZMAREK, L. K. & ZUCKER, R. S. (2001). Presynaptic target of Ca^{2+} action on neuropeptide and acetylcholine release in *Aplysia californica*. *Journal of Physiology* (in the Press).
- PITLER, T. A. & ALGER, B. E. (1992). Postsynaptic spike firing reduces synaptic GABA_A responses in hippocampal pyramidal cells. *Journal of Neuroscience* **12**, 4122–4132.
- PITLER, T. A. & ALGER, B. E. (1994). Depolarization-induced suppression of GABAergic inhibition in rat hippocampal pyramidal cells: G protein involvement in a presynaptic mechanism. *Nature* **13**, 1447–1455.
- REGEHR, W. G. & TANK, D. W. (1992). Calcium concentration dynamics produced by synaptic activation of CA1 hippocampal pyramidal cells. *Journal of Neuroscience* **12**, 4202–4223.
- TANG, Y., SCHLUMBERGER, T., KIM, T., LUEKER, M. & ZUCKER, R. S. (2000). Effects of mobile buffers on facilitation: experimental and computational studies. *Biophysical Journal* **78**, 2735–2751.
- VINCENT, P. & MARTY, A. (1993). Neighboring cerebellar Purkinje cells communicate via retrograde inhibition of common presynaptic interneurons. *Nature* **11**, 885–893.
- VON GERSDORFF, H. & MATTHEWS, G. (1994). Inhibition of endocytosis by elevated internal calcium in a synaptic terminal. *Nature* **370**, 652–655.
- WILSON, R. I. & NICOLL, R. A. (2001). Endogenous cannabinoids mediate retrograde signaling at hippocampal synapses. *Nature* **410**, 588–592.
- ZHAO, M., HOLLINGWORTH, S. & BAYLOR, S. M. (1996). Properties of tri- and tetracarboxylate Ca^{2+} indicators in frog skeletal muscle fibers. *Biophysical Journal* **70**, 896–916.
- ZUCKER, R. S. (1993). The calcium concentration clamp: spikes and reversible pulses using the photolabile chelator DM-nitrophen. *Cell Calcium* **14**, 87–100.
- ZUCKER, R. S. (1994). Photorelease techniques for raising or lowering intracellular Ca^{2+} . *Methods in Cell Biology* **40**, 31–63.
- ZUCKER, R. S. (1996). Exocytosis: a molecular and physiological perspective. *Nature* **17**, 1049–1055.

Acknowledgements

We thank Rachel Wilson for valuable technical advice. This work was supported by NIH Grant NS 15114.

Corresponding author

R. S. Zucker: Molecular and Cell Biology Department, 111 Life Sciences Addition, University of California, Berkeley, CA 94720-3200, USA.

Email: zucker@socrates.berkeley.edu